Carbohydrate Polymers 254 (2021) 117371

Contents lists available at ScienceDirect

Carbohydrate Polymers

journal homepage: www.elsevier.com/locate/carbpol

Structural characterization and immunological activity of pectin polysaccharide from kiwano (*Cucumis metuliferus*) peels

Minqian Zhu, Riming Huang, Peng Wen *, Ya Song, Baolin He, Jialing Tan, Huili Hao, Hong Wang *

Guangdong Provincial Key Laboratory of Food Quality and Safety, College of Food Science, South China Agricultural University, Guangzhou 510642, China

ARTICLE INFO

Keywords:
Kiwano (*Cucumis metuliferus*) peels
Pectin polysaccharide
Structural characterization
Immunological activity

ABSTRACT

Two novel polysaccharides, namely CMPP-1 and CMPP-2, from kiwano (*Cucumis metuliferus*) peels were isolated through hot-water extraction, followed by ethanol precipitation and column chromatography. The results showed that CMPP-1 and CMPP-2 were hetero-galacturonans with different molecular weights of 7.35 kDa and 6.90 kDa, respectively. Both of CMPP-1 and CMPP-2 were mainly composed of glucuronic acid (45.93 % and 51.75 %, respectively), and other monosaccharides including rhamnose, arabinose, galactose, glucose, xylose, fucose, mannose, galacturonic acid, and mannuronic acid. The results of structural characterization from FT-IR and NMR confirmed that CMPP-1 and CMPP-2 were pectin with highly branched structure. Furthermore, both CMPP-1 and CMPP-2 possessed immune-enhancing activity and could enhance the secretion of nitric oxide and cytokines (TNF-α, IL-6) in a dose-dependent manner. Especially, CMPP-1 had higher immune activity than CMPP-2 as the minimum effective concentration were 0.78 μg/mL and 6.25 μg/mL, respectively. These findings provide a scientific basis for further utilization of polysaccharide from kiwano peels.

1. Introduction

Polysaccharides come from a wide range of sources and have many biological activities, such as antimicrobial activity, anti-inflammatory, antioxidant activity, anti-diabetic activity, immunoregulatory *etc* (Ullah, Khalil, Shaukat, & Song, 2019). Among which, pectin is an immunologically active polysaccharide which widely presents in plants, and has various functions with high safety (Mohnen, 2008). Recently, the studies on pectin activity become the research hotspot. For example, the pectin polysaccharides from sweet cherry (Cao et al., 2018), mulberry (Wang, Li et al., 2018) and pomegranate peels (Gavlighi, Tabarsa, You, Surayot, & Ghaderi-Ghahfarokhi, 2018), which were effective in inducing NO and TNF-α release from RAW264.7 cells. However, not all pectin polysaccharides have the immune regulation activity (Cao et al., 2018), such as pectin from *Achillea millefolium* (Freysdottir, Logadottir, Omarsdottir, Vikingsson, & Hardardottir, 2016). Therefore, the new pectin polysaccharide is worthy of further development.

Kiwano (*Cucumis metuliferus*), one kind of the genus *Cucurbitaceae*, has been served as bioactive compounds for hypoglycemic (Gotep, 2011), anti-ulcer (Omale, Wuyep, Auta, & Wannang, 2011), antifungal (Nwadiaro, Ogbonna, Wuyep, & Sila-Gyang, 2015), antiviral (Anyanwu & Wannang, 2014), etc. Though kiwano becomes popular fruit and has the potential for fully commercialization, the research on kiwano peels was rarely. The peels are by-products of the juice extraction process which weighs accounts for about a quarter of the total fruit. It has been reported that kiwano peels showed strong ferrous ion-chelating capacity (Matsusaka & Kawabata, 2010), indicating biological activity. Several pectin polysaccharides obtained from fruits peels, such as sweet lemon peel (Rahmani, Khodaiyan, Kazemi, & Sharifan, 2019), pistachio green hull (Kazemi, Khodaiyan, Labbafi, Hosseini, & Hojjati, 2019) and watermelon rind (Dammak et al., 2019). These pectin were mainly composed galacturonic acid, galacturonic, arabinose, rhamnose, et al., with HG and RG-I domains, which the structures were associated with immune activity (Popov & Ovodov, 2013). Although some pectin obtained from fruits of genus *Cucumis*, like *Cucumis melo* (Denman & Morris, 2015) and *Cucumis sativus* (Chen, Huang, & Huang, 2019), there were no studies on polysaccharides from *Cucumis metuliferus* peels.

In order to investigate the bioactivity of the polysaccharides from kiwano peels, two novel polysaccharides fractions (CMPP-1 and CMPP-2) were prepared by a series of extraction and purification. The chemical

* Corresponding authors.
E-mail addresses: zhuminqian@stu.scau.edu.cn (M. Zhu), huangriming@scau.edu.cn (R. Huang), wenpeng100@163.com (P. Wen), songya_1990@163.com (Y. Song), hebaolin@scau.edu.cn (B. He), 995340450@qq.com (J. Tan), hhlhaohuili@stu.scau.edu.cn (H. Hao), gzwhongd@163.com (H. Wang).

https://doi.org/10.1016/j.carbpol.2020.117371
Received 16 July 2020; Received in revised form 6 October 2020; Accepted 30 October 2020
Available online 24 November 2020
0144-8617/

structure of polysaccharides was elucidated using fourier transform-infrared spectroscopy (FT-IR), gel permeation chromatography (GPC), high-performance anion-exchange chromatography with pulsed amperometric detection (HPAEC-PAD), and nuclear magnetic resonance (NMR) spectroscopy. Moreover, the immune-enhancing activities of CMPP-1 and CMPP-2 were evaluated to investigate the effects on cell viability, production of nitric oxide (NO) and secretion of cytokines (TNF-α and IL-6) on RAW264.7 macrophages cells.

2. Materials and methods

2.1. Materials and reagents

Kiwanos were purchased from a supermarket in Fujian province in China. The peels were removed manually and washed with distilled water, after then which were freeze-dried. The peels were ground by using a blender, passed through a 0.5 mm sieve and kept in seal sample bags (No. 20180208) at −80 °C in Guangdong Provincial Key Laboratory of Food Quality and Safety, South China Agricultural University, China.

DEAE-52 cellulose, Sephadex G-100 and lipopolysaccharide (LPS) were purchased from Shanghai Yuanye Bio-Technology Co. LTD (Shanghai, China). Standard monosaccharides (glucose, galactose, arabinose, rhamnose, fucose, xylose, mannose, ribose, galacturonic acid, and glucuronic acid) were purchased from Sigma Co. (MO, USA). Acetonitrile and trifluoroacetic acid (TFA) were of chromatographic grade from Sigma-Aldrich Co. LLC. (St. Louis, MO, USA).

RAW264.7 murine macrophage cells were obtained from American Type Culture Collection (ATCC, Manassas, VA, USA). Dulbecco's modified Eagle's medium (DMEM), fetal bovine serum (FBS) penicillin-streptomycin and trypsin were the products of Gibco BRL (Gaithersburg, MD, USA). NO detection kit was purchased from Beyotime Institute of Biotechnology (Jiangsu, China). TNF-α and IL-6 enzyme linked immunosorbent assay (ELISA) kits were purchased from NeoBioscience Biotechnology Co. LTD (Shenzhen, China). All other reagents used in this study were of analytical grade.

2.2. Polysaccharide extraction and purification

The dried peel powder was mixed with distilled water, at the ratio of 1:30 (w/v), stirred and heated to 70 °C for 3 h. The extractive was filtered and centrifuged at 12,000 rpm for 15 min to collect the supernatant, and the precipitation was mixed with distilled water to repeat the extraction. The supernatant of two extractions were combined and concentrated to 10 % of the original volume by a rotary evaporator at 65 □, and then mixed with Sevag reagent (CHC_{l3}: n-C_4H_9OH = 4:1, v/v) in a volume ratio of 4:1 followed by centrifuging at 12,000 rpm for 15 min to remove protein. Then the supernatant was mixed with four volumes of 95 % ethanol overnight at 4 ℃ and centrifuged at 12,000 rpm for 15 min. The precipitate was re-dissolved and dialyzed against distilled water (molecular weight cut off 5 kDa) for 3 days. Finally, the dialysate was collected and lyophilized to obtain the crude polysaccharide of *C. meluliferus* peels (CMPP).

The CMPP was dissolved in distilled water and loaded on a Cellulose DEAE-52 column (4.5 × 70 cm) for further purification. Distilled water and 0.1−0.5 mol/mL of gradient sodium chloride (NaCl) solution were used to fractionate and elute the column at a flow rate of 3 mL/min, 10 mL per tube. Each fraction was gathered and measured by the phenol-sulfuric acid method (Dubois, Gilles, Hamilton, Rebers, & Smith, 1956) to assay the content of carbohydrate. The water eluent was further purified with the Cellulose DEAE-52 column, and the main polysaccharide fraction was collected, dialyzed and lyophilized. The polysaccharides obtained above were further fractionated using Sepharose G-100 column (2.5 cm × 90 cm) and equilibrated with distilled water at a flow rate of 0.5 mL/min, 5 mL per tube. The eluate was analyzed using the phenol-sulphuric acid assay, and the fractions were collected separately.

2.3. Purity assessment and molecular weight analysis

The total flavones in the polysaccharide were determined by the Sodium Nitrite-Aluminum Nitrate (Wang, Zheng, Cai, Yuan, & Gong, 2018), the total phenolics in the polysaccharide were determined by the Folin-Ciocalteus method (Zhang et al., 2008). The UV–vis spectrum of the water solution of the sample (1 mg/mL) was measured on a DU-8000 spectrophotometer (NanoDrop 2000c, Thermo Fisher Scientific, MMAS, USA) in a wavelength range of 190−800 nm.

The homogeneity and molecular weight of polysaccharides were determined by gel permeation chromatography (GPC) in a Waters 1525 HPLC system coupled with Waters 2414 differential refractive index detector, using TSK G-5000 PWXL column (7.8 mm × 300 mm) and TSK G-3000 PWXL column (7.8 mm × 300 mm). The Potassium dihydrogen phosphate (0.02 mol/L) was used as eluent at a flow rate of 0.6 mL/min with the column temperature maintained at 35 ± 0.1 °C and 10 μL samples (3 mg/mL) was injected for each run. The linear regression was calibrated with T-series dextran standards and the molecular weights (eight standards of 1 × 10^3-1 × 10^7 Da) of the polysaccharide was expressed as the dextran equivalent molecular weight.

2.4. Monosaccharide analysis

5 mg polysaccharide sample was hydrolyzed using 1 mL 2.5 mol/L TFA at 121 °C for 2 h. Using nitrogen gas with the methanol to remove the excess TFA three times, then the dried samples were dissolved with distilled water and prepared for injecting to the high-performance anion-exchange chromatography with pulsed amperometric detection (HPAEC-PAD) which was consist of ICS-5000 system (Thermo Fisher Scientific) equipped with Dionex™ CarboPac™ PA20 (150 mm × 3 mm, 6.5 μm) and pulsed amperometric detector.

2.5. Congo red analysis and Scanning Electron Microscope (SEM)

Sample (0.5 mg/mL, 1 mL) mixed with the Congo red reagent (0.01 %, 2 mL). The NaOH concentration in the solution gradually increased from 0 to 0.5 mol/mL, and the maximum absorption wavelength at each NaOH concentration was recorded in the process with an ultraviolet-visible spectrophotometer. The Congo red solution without polysaccharide was used as control (Zhang et al., 2019).

The scanning electron micrograph of samples were obtained using an environmental scanning electron microscope (LEO1530VP, Zeiss, Oberkochen, Germany). The dried powder sample was placed on a specimen holder fixed with double-sided adhesive tape, then sputtered with gold powder using a sputter coater and observed at 500 × and 5000× magnifications.

2.6. Fourier transform infrared spectroscopy (FT-IR)

For FI-IR analysis, 1 mg of the sample mixed with KBr powder, ground and then pressed into 1 mm pellets for Fourier transform infrared (FT-IR) measurement (Bruker, Rheinstetten, Germany). FT-IR spectra of the polysaccharide was measured in the frequency range of 4000–400 cm^{-1}.

2.7. Methylation analysis

The reduction of uronic acids of the polysaccharides were performed by using the method of methylation. The samples (10 ± 0.05 mg) were reduced with $NaBH_4$ and $NaBD_4$, dialyzing and lyophilizing to acquire the reduzates, the reduzates were methylated in DMSO/NaOH with CH_3I. After complete methylation, the permethylated products were hydrolyzed with 2 mol/L TFA at 121 °C for 1.5 h, reduced by $NaBD_4$ and acetylated with acetic anhydride. The acetates were dissolved in chloroform and analyzed with GC–MS on an Agilent 6890A-5975C equipped with Agilent BPX70 chromatographic column (California, USA). The

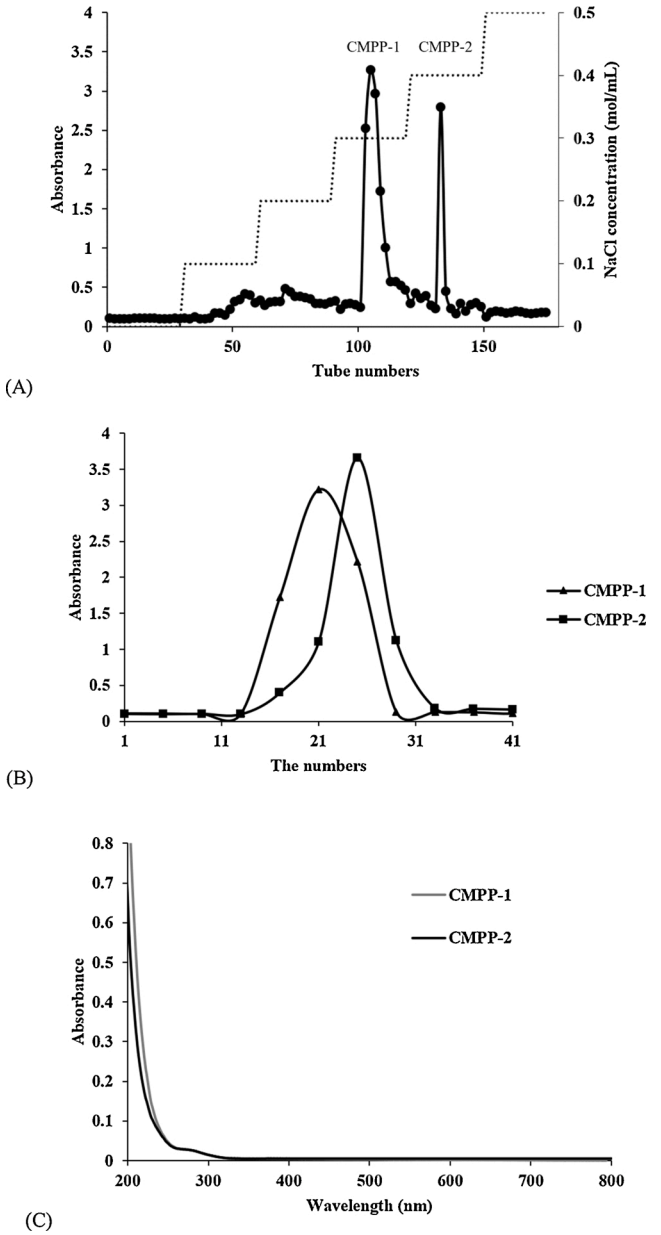

Fig. 1. Separation of CMPP-1 and CMPP-2. DEAE-cellulose elution curve (A); Sephadex G-100 elution curve (B). General properties of CMPP-1 and CMPP-2. UV–vis spectrum (C).

column temperature was started with 140 °C and held for 2 min, increasing by 3 °C /min to 230 °C and hold for 3 min. The injection temperature was 260 °C and detector temperature was 230 °C. Helium was used as the carrier gas with 1 mL/min. Mass spectra was interpreted to identify the compound that corresponded to each peak, and the relative molar ratio was calculated according to equation:

Relative molar ratio (%) = relative molar quantity/sum of relative molar quantities of each component; (1)

Relative molar quantity = molecular weight/peak area. (2)

Table 1
Monosaccharide composition of CMPP-1 and CMPP-2.

Monosaccharide	CMPP-1	CMPP-2
Monosaccharide composition (%)		
GalA	45.93	51.75
Rha	13.50	16.24
Gal	13.81	9.57
Ara	10.37	5.79
Glu	5.54	4.67
Xyl	4.24	8.05
Fuc	2.51	2.03
GluA	2.07	1.00
ManA	1.79	0.51
Man	0.17	0.32
Molar ratio[a]		
HG (%)	32.43	35.51
RG-I (%)	51.18	47.84
R1	1.03	1.24
R2	0.29	0.31
R3	1.79	0.95

[a] Molar ratios: exhibiting the primary structural properties of pectin molecules; HG= GalA – Rha, homogalacturonan; RG-I = 2Rha + Ara + Gal, rhamenogalacturonan-I; R1=GalA/(Fuc+Rha+GluA+Ara+Gla+Xyl), the linearity of pectin; R2=Rha/GalA, the contribution of RG to pectin population; R3= (Gal+Ara)/Rha, the length of side chains attached to RG-I.

2.8. Nuclear magnetic resonance (NMR) spectroscopy

For the NMR spectroscopy, 30 mg of the sample was dissolved in 0.5 mL D_2O to a final concentration of 60 mg/mL. 1D-NMR and 2D-NMR (^{1}H-NMR, ^{13}C-NMR, COSY and HSQC) were recorded at 25 ℃ with a Bruker AVANCE IIIHD 600 spectrometer system (Bruker, Rheinstetten, Germany) operating at 600 MHz. Chemical shifts were expressed in ppm relative to acetone at δ 2.22/30.2 (^{1}H /^{13}C).

2.9. Immunomodulatory activity

2.9.1. Cell culture and reagents

Murine macrophage RAW264.7 cells were grown in Dulbecco modified Eagle's medium (DMEM) with 10 % heat-inactivated fetal bovine serum (FBS) and 1% penicillin and streptomycin. All cultures were performed in culture plates at 37 °C in a humidified atmosphere containing 5 % CO_2.

2.9.2. Cell viability assay

Cell viability was determined by 3-(4,5-Dimethylthiazol-2-yl)-2,5-bromo diphenyltetrazolium (MTT) method, where the reduction of crystal tetrazolium forming through mitochondrial enzymes was possible only in viable cells. Cells were plated in 96 well plates (3×10^4 cells/well) and treated with different concentrations of polysaccharides. After 24 h, 10 μL/well of the 5 mg/mL MTT solution was added. After 4 h of incubation, the cell supernatant was moved and 100 μL of Dimethylsufoxide (DMSO) was added for lysis and crystal solubilization. Then absorbance was recorded 490 nm wavelength.

2.9.3. Assay of NO and cytokine production

RAW264.7 cells were plated onto 24 well plates (5×10^5 cells/100 μL), induced with 1 μg/mL LPS (for the positive group), FBS (as the control group) or different concentration of polysaccharides at 37 °C for 24 h. The NO production was assayed using the Griess reagent and absorbance was recorded 540 nm wavelength. The other media was collected and diluted to an appropriate concentration for ELISA that absorbance was subsequently read at 540 nm. Three independent experiments were performed with three parallel wells in each experiment.

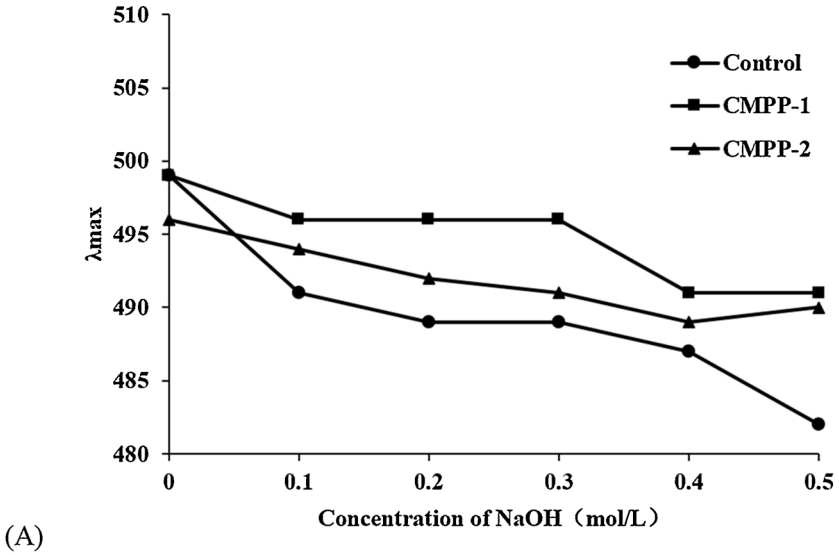

(A)

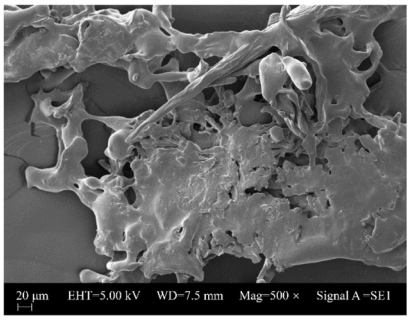

(B)

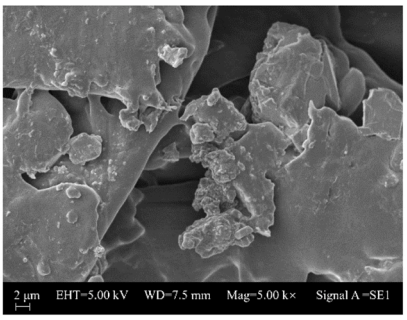

(C)

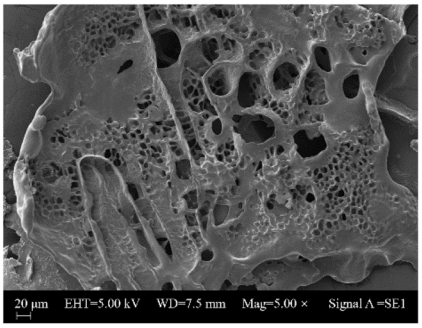

(D)

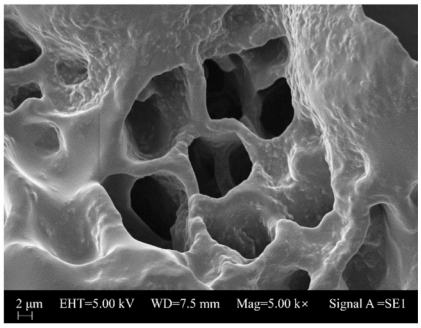

(E)

Fig. 2. Triple helical conformation analysis of CMPP-1 and CMPP-2 (A); SEM images of CMPP-1 (B: ×500; C: ×5k) and CMPP-2 (D: ×500; E: ×5k).

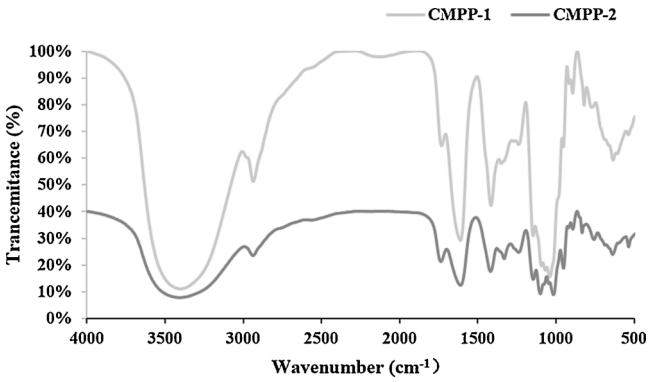

Fig. 3. FT-IR spectrum of CMPP-1 and CMPP-2.

2.10. Statistical analysis

All experiments were repeated in triplicate. Data of immunomodulatory activity were expressed as mean ± standard deviations (SD). Significance was analyzed by one-way ANOVA using SPSS 20.0 software (IBM Corporation, Armonk, NY, USA). Comparisons with $p < 0.05$ were considered significant differences.

3. Results and discussion

3.1. Preparation and purification analysis

First, the crude polysaccharide (CMPP) from kiwano peels was obtained by hot water extraction and ethanol precipitation. Then, the CMPP was separated on a Cellulose DEAE-52 chromatography, and the separation flow diagram was illustrated in Fig. 1(A). Two main fractions eluted by 0.3 and 0.4 mol/L NaCl were collected, designating CMPP-1 and CMPP-2, respectively. After that, the two fractions were desalted and further purified by a Sepharose G-100 column. As a result, a single and symmetrical elution peak was apparent from the two eluents (Fig. 1B). After the purification, the total flavones and total polyphenols were not detected, and Fig. 1(C) showed no absorbance at 260 nm and 280 nm which indicated no nucleic acid and protein existed (Morrison & Jacobs, 1976). Furthermore, based on the calibration curve between retention time and the logarithm of Mw of dextran standards, CMPP-1 and CMPP-2 had a homogeneous Mw distribution of 7.35 kDa and 6.90 kDa, respectively, which was more than that of pistachio hull (1.66 kg/mol) (Kazemi et al., 2019), but less than that of lemon peel (615.836 kg/mol) (Rahmani et al., 2019). The result indicated the high Mw in molecular sizes of CMPP-1 and CMPP-2.

3.2. Monosaccharide analysis

Polysaccharides are comprised of monosaccharides, which also influence the structure and activity of polysaccharides. For understanding the monosaccharides composition and degree of branching, the monosaccharide content of each fraction was determined by HPAEC-PAD. As showed in Table 1, both CMPP-1 and CMPP-2 had mainly 10 monosaccharides composition, including GalA, Rha, Ara, Gal, Glu, Xyl, Fuc, GluA, ManA and Man, in differences ratios. GalA was the main constituent as the linear chains in the structure of CMPP-1 and CMPP-2 with a value of 45.93 % and 51.75 %, respectively. Rha, Gal and Ara accounted for more than half of total neutral sugars which suggested the high amount of RG-I in the two fractions structure. The value of HG (32.43 %/35.51 %) was less than that of RG-I (51.18 %/47.84 %), which exhibited the part of linear was less than the part of side chains in CMPP-1 and CMPP-2, respectively. It was reported that pectin containing less than 75 % galacturonic acid residues and ramified region, especially the RG-I fragment of the branched region, were shown to play an important role in stimulating the immune response (Popov and Ovodov, 2013). In the current study, the R1value of the each fraction (1.03/1.24) was found to be lower than sweet lemon peel (1.53) (Rahmani et al., 2019), grapefruit peel pectin (2.52) (Wang et al., 2016) and pistachio green hull pectin (1.97) (Kazemi et al., 2019), means the CMPP-1 and CMPP-2 had more part of side chains than them. Besides, the R2 and R3 value indicated that the two components were mainly RG-I domain, and the degree of branching in CMPP-1 was higher than CMPP-2.

3.3. Morphological properties

In generally, the triple helix structure is considered to be related to biological activity (Liu & Xu, 2016). As shown in Fig. 2(A), there was no triple helix structure in the two fractions with the concentration range of 0–0.5 mol/L NaCl, similar to the polysaccharide from fermented Apple Pomace (Feng, YuRong, Xi, Dong, & Jie, 2017). It was reported that the polysaccharide with molecular weight less than 90 kDa usually had not the triple helix structure, corresponding to the molecular weight analysis of the results in previous research (Hazime et al., 1991).

The molecular morphology of polysaccharides was investigated by SEM under 500 × and 5000 × magnifications (Fig. 2B–E). The CMPP-1 was an irregular block with a smooth surface, while CMPP-2 occurred in a state of aggregation with network structures. CMPP-2 had more circular cavity, which might because it existed the repulsive forces in the polysaccharide molecules, leading to weak intermolecular attractiveness (Li, Zhong, & Liu, 2010). The differences in surface morphology might ascribe to the different degrees of branching in the two fractions.

3.4. FI-IR analysis

The chemical bonds and functional groups of CMPP3 and CMPP4 were further analyzed by FT-IR (Fig. 3). The broadly-stretched intense peak at around 3300–3500 cm^{-1} represented the stretching of the hydroxyl groups, and the small peaks observed at around 2920 cm^{-1} was attributed to the CH stretching and bending vibrations of free sugars (Jiao, Kuang, Hu, & Chen, 2018). The ester carbonyl C═O asymmetric stretching vibration at 1730 cm^{-1} indicated the existence of acetylation, the non-ester carbonyl C═O asymmetric stretching vibration at 1610 cm^{-1} suggested the existence of uronic acid (Shu et al., 2018). The absorption peak at 1240 cm^{-1} was also assigned to the trace of uronic acids and ester sulfate (Jiao, Hua, Dong, Qian, & Yan, 2018). Furthermore, the 1200–950 cm^{-1} was dominated by ring vibrations overlapped with stretching vibrations of the C—OH— side groups and the C—OC— glycosidic bond vibration. The strong absorbance of at 1017 cm^{-1} and 1101 cm^{-1} attributed to the stretching vibrations of the pyranose ring of the glucosyl residue (Ren, Zhao, Zheng, Alim, & Yang, 2019). It had different bending vibrations of peaks between CMPP-1 and CMPP-2, which may be related to the number of functional groups in each fraction. Moreover, the absorptions at about 825 and 895 cm^{-1} indicated that α- and β-configurations were both present (Bi et al., 2018). Consequently, the results suggested that the structure of CMPP-1 and CMPP-2 contained the typical groups of pectin.

3.5. Methylation analysis

To further obtain the structural information of CMPP-1 and CMPP-2, the glycosidic bond types were analyzed by methylation and GC–MS methods. As summarized in Table 2, the results demonstrated that CMPP-1 and CMPP-2 were identified as nine and eleven derivatives, respectively. Among these monosaccharide residues, CMPP-1 and CMPP-2 had four same types of glycosidic bond at different relative

Table 2
Methylate analysis data of CMPP-1 and CMPP-2.

Retention Time (min)	Type of Linkage	Methylated Sugars	Relative Molar Ratios (%)[a]	Mass Fragments
CMPP-1				
6.537	t-Ara(*f*)	2,3,4-Me3-Ara	6.84	87,102,118,145,161
9.514	2-Rha(*p*)	3,4-Me2-Rha	16.02	72,89,115,131,160,190,234
9.719	4-Rha(*p*)	2,3-Me2-Rha	3.72	71,101,118,162,202,234
10.712	t-Gal(*p*)A	2,3,4,6-Me4-Gal	14.53	55,71,87,118,161,205,220,263
11.375	5-Ara(*f*)	2,3-Me2-Ara	2.87	71,87,102,118,162,189
14.653	4-Gal(*p*)A	2,4,6-Me3-Gal	40.20	71,118,173,203,233
16.679	3,4-Gal(*p*)	2,6-Me2-Gal	7.86	59,87,118,185,232,305
17.904	2,4-Gal(*p*)	3,6-Me2-Gal	4.66	71,88,113,130,173,190,211,233,274
19.69	4,6-Gal(*p*)	2,3-Me2-Gal	3.30	71,85,118,159,201,261,299,338
CMPP-2				
6.264	t-Rha(*p*)	2,3,4-Me3-Rha	3.58	59,72,89,102,131,162
7.927	t-Ara(*p*)	2,3,4-Me3-Ara	5.55	59,88,118,129,161,173
9.535	2-Rha(*p*)	3,4-Me2-Rha	24.35	57,72,89,100,131,160,190
9.678	t-Glu(*p*)	2,3,4,6-Me4-Glu	5.46	71,102,145,162,205,234
10.712	t-Gal(*p*)A	2,3,4,6-Me4-Gal	7.82	71,87,102,118,145,161,205
13.264	2,4-Rha(*p*)	3-Me-Rha	3.75	74,88,130,160,190
13.73	3-Gal(*p*)	2,4,6-Me3-Gal	2.39	87,101,118,161,203,234,277
14.688	4-Gal(*p*)A	2,3,6-Me3-Gal	35.71	71,118,173,203,233
14.941	4-Glu(*p*)	2,3,6-Me3-Glu	3.30	71,118,162,203,233
16.672	3,4-Gal(*p*)A	2,6-Me2-Gal	6.00	59,87,118,185,232,305
17.883	2,4-Gal(*p*)	3,6-Me2-Gal	2.10	71,88,113,130,173,190,214,233,27

[a] Relative molar ratio (%) = relative molar quantity/sum of relative molar quantities of each component; Relative molar quantity = molecular weight/peak area.

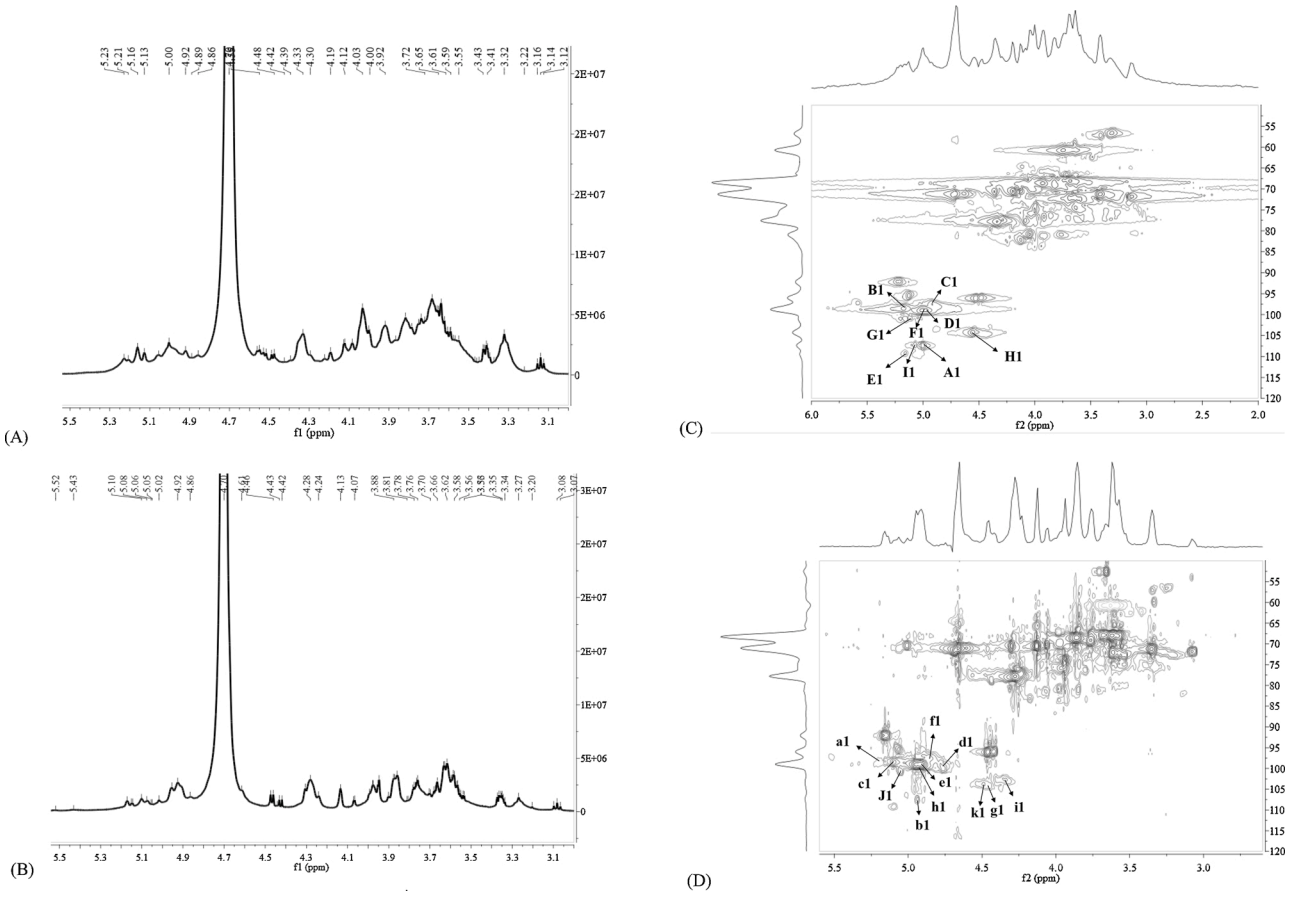

Fig. 4. ^{1}H NMR spectrum (A-B) and HSQC spectrum (C-D) of CMPP-1 and CMPP-2.

molar ratios, respectively, including →2)-Rha*p*-(1→, t-Gal*p*A-(→1, →4)-Gal*p*A-(1→ and →2,4)-Gal*p*-(1→. GalA residues of two fractions were in accordance with monosaccharide composition analysis, and →4)-Gal*p*A-(1→ were consider as the major building blocks, consistent with the most of pectin polysaccharides. It's well known that pectin had several domains like HG, RG-I and RG-II, etc, and the differences in structure of pectin polysaccharides were the ratio of domains and the branching of the side chains (Mohnen, 2008). Therefore, in addition to the differences of relative molar ratios in the two fractions, the glycosidic bond types may also be the cause of structural differences among CMPP-1 and

Table 3
Chemical shift assignment of glycosidic linkages in CMPP-1 and CMPP-2.

Residues Linkage		H1/C1	H2/C2	H3/C3	H4/C4	H5/C5	H6/C6
CMPP-1							
A α-L-Ara*f*	H	4.99	4.04	3.82	4.12	3.71/3.80	
	C	107.26	80.65	76.25	82.21	60.74	
B	H	5.16	4.32	3.91	3.41	3.68	1.15
2)-α-L-Rha*p*	C	98.66	77.50	69.50	71.37	68.32	16.35
C	H	4.92	3.99	4.03	3.92	3.68	1.15
2,4-α-L-Rha*p*	C	97.41	75.17	69.51	81.13	68.13	16.35
D	H	4.97	3.40	3.63	3.37	3.99	
α-D-Gal*p*A	C	98.79	71.37	72.23	69.47	75.00	174.73
E	H	5.15	4.11	4.08	4.22	3.91/3.84	
5)-α-L-Ara*f*	C	108.99	82.04	75.17	81.26	68.60	
F	H	5.00	3.66	3.82	4.33	4.68	
4)-α-D-Gal*p*A	C	98.66	67.96	68.91	77.50	71.24	174.73
G	H	5.05	3.66	3.93	4.10	3.69	3.74
3,4-α-D-Gal*p*	C	100.82	72.19	81.13	80.78	76.84	60.61
H	H	4.54	3.58	3.82	4.11	3.66	3.74/3.82
4)-β-D-Gal*p*	C	104.28	74.24	76.12	77.89	74.52	60.44
I	H	5.07	4.08	3.72	3.53	3.85	3.63
4,6)-β-D-Gal*p*	C	107.26	77.37	76.72	76.25	68.91	68.13
CMPP-2							
a	H	5.16	4.13	3.75	3.35	4.05	1.33
α-L-Rha*p*	C	98.32	70.53	72.91	71.23	70.2	16.25
b	H	4.92	4.06	3.84	4.17	3.60	3.86
α-L-Ara*p*	C	107.43	81.4	75.14	83.2	65.39	68.30
c	H	5.09	4.27	3.96	3.35	3.62	1.09
2)-α-L-Rha*p*	C	98.79	77.72	69.77	71.24	67.66	16.10
d	H	4.76	3.58	3.62	3.84	3.97	3.56
β-D-Glu*p*	C	99.92	72.20	72.04	70.67	69.88	63.12
e	H	4.94	3.34	3.61	3.20	3.93	
α-D-Gal*p*A	C	99.02	68.70	72.12	71.81	74.08	175.06
f	H	4.86	3.85	4.07	3.85	3.67	1.15
2,4-α-Rha*p*	C	97.45	74.86	70.40	81.24	67.96	16.38
g	H	4.47	3.75	3.93	4.30	3.80	3.60
3)-β-D-Gal*p*	C	103.95	72.75	81.95	70.64	76.12	63.00
h	H	4.91	3.61	3.87	4.27	4.68	
4)-α-Gal*p*A	C	98.96	68.17	68.44	77.76	71.11	175.06
i	H	4.37	3.84	3.76	3.57	3.57	3.75
4)-β-D-Glu*p*	C	102.70	74.75	72.63	80.15	72.20	63.86
j	H	5.05	3.67	4.24	4.44	5.00	
3,4)-α-D-Gal*p*A	C	100.69	67.90	77.72	78.62	70.40	170.76
k	H	4.53	3.64	3.84	4.12	3.62	3.77/3.86
4)-β-D-Gal*p*	C	103.67	72.02	77.20	76.25	74.87	61.69

CMPP-2.

3.6. NMR analysis

To further interpret the structure of CMPP-1 and CMPP-2, the polysaccharides were analyzed via 1D-NMR and 2D-NMR. The ^{1}HNMR spectra of the two fractions represented were showed in Fig. 4(A–B). In the ^{1}H NMR spectra, the majority of signals appeared within 3.2–5.1 ppm. The chemical shift was influenced by the sugar type, linkage type, substitution and modifications. In general, the anomeric signals over 4.9 ppm region represented the type of α-configuration and less than 4.9 ppm represented β-configuration (Song et al., 2019). Thus, it can be concluded that the two fractions both have α- and β- configuration.

Combined with the methylation analysis and HSQC spectra (Fig. 4C–D), the chemical shifts of these glycosidic linkages in CMPP-1 and CMPP-2 were assigned and listed in Table 3. Gal*p*A residues were expected to be the most abundant residues. CMPP-1 and CMPP-2 both had two similar anomeric signals at 4.92/4.94 and 5.00/4.91 ppm, and carbon signals at 99.02/98.75 and 98.96/08.66, which were assigned to α-D-Gal*p*A-1 and 4-D-Gal*p*A-1 (Mei, Yang, Zhu, Peng, & Liang, 2014; Yi et al., 2016). While CMPP-2 had anomeric proton signals and carbon signals at 5.05 and 100.69 that were assigned to 3,4-α-D-Gal*p*A-1 (Yang et al., 2018). The chemical shifts of CMPP-1 and CMPP-2 consistent nearly with the reported values, and it could be deduced that the backbones of CMPP-1 and CMPP-2 were proven to have the HG domain. The anomeric signals at 5.16/5.09 and 4.92/4.86 ppm, and carbon signals at 98.66/98.79 and 97.41/97.45 were corresponded to the 2-α-L-Rha*p*-1 and 2,4-α-L-Rha*p*-1 in CMPP-1 and CMPP-2, respectively, similar to the features of RG-I domains (Liu, Zhao, Wu, John, & Yang, 2017; Liu, Liu, Zhu, Yu, & Gaoa, 2016). As literatures reviewed, the structure of CMPP-1 and CMPP-2 can be divided linear HG regions and branched rhamnogalacturonan RG-I regions.

Considering the results of methylation analysis, the NMR signals indicated the presence of same residues in repetitive units of CMPP-1 and CMPP-2. The signal at 4.54/4.53 and 104.28/103.67 were attributed to 2,4-Gal*p*-1 in CMPP-1 and CMPP-2, respectively (Liu et al., 2017). However, there were also differences in glycosidic bond types of the two fractions. The anomeric and carbon signal at 5.05/100.82 and 5.07/107.26 were assigned to 3,4-α-D-Gal*p* and 4,6)-β-D-Gal*p* in CMPP-1, while the signal at 4.47/103.95 was assigned to 3)-β-D-Gal*p* in CMPP-2 (Du, Li, Zhu, Huang, & Yu, 2018; Molaei & Jahanbin, 2018; Wei et al., 2019). The signal at 4.99/107.26 and 5.15/108.99 were appointed to α-L-Ara*f* and 5)-α-L-Ara*f* in CMPP-1, and the signal appeared in 4.92/107.43 was appointed to α-L-Ara*p* in CMPP-2 (Jiao, Hua et al., 2018; Yang et al., 2018). Especially, the β-D-Glu*p* and 4)-β-D-Glu*p* were only detected in CMPP-2, which were matched with the signal of 4.76/99.92 and 5.05/102.7 (Lei et al., 2018; Zhao et al., 2014). These results may be concluded that the two fractions have difference glycosidic bond types in branches of side chain.

Combined with methylation and above NMR analysis, the backbone chain of CMPP-1 and CMPP-2 were composed by repeated 4-α-D-Gal*p*A-1, and portion of region was linked by 4-α-D-Gal*p*A-1 and 2-α-L-Rha*p*-1 alternatively. Furthermore, CMPP-1 had a branch of 2,4)-Gal*p*-(1, 3,4)-α-D-Gal*p*-(1, 4,6)-β-D-Gal, α-L-Ara*f* and 5)-α-L-Ara*f*, while CMPP-2 had 2,4)-Gal*p*-(1, 3)-β-D-Gal*p*, α-L-Ara*p*, β-D-Glu*p*-(1, β-D-Glu*p* and 4)-β-D-Glu*p*. The probable structure detail of CMPP-1 and CMPP-2 were designed in Fig. 5(A–B). These structures of the two fractions were similar to the pectin polysaccharides from *Cucumis melo* (Denman et al., 2015), which also had HG and RG-I domains, and the branches were consists of Gal and Ara, etc. Besides, compared with CMPP-2, CMPP-1 had more glycoside bonds with connection points, which suggested the branching degree of CMPP-1 was higher than CMPP-2, corresponding to monosaccharide composition analysis.

3.7. Cell viability

The cytotoxicity of polysaccharides was evaluated against RAW264.7 macrophages by MTT assay (J. Du et al., 2018). As shown in Fig. 6, CMPP-1 and CMPP-2 exhibited no inhibition on cell viability under the concentration of 50 μg/mL for 24 h. It should be noted that the cell viability was significant enhanced ($p < 0.05$) at the concentration range of 0.78–3.13 μg/mL for CMPP-1 and 12.5–25 μg/mL of CMPP-2, respectively, which were the optimum concentration ranges. Considering the polysaccharides from *Dendrobium officinale* (Zeng, Yang, Wang, Zong, & Lou, 2019) and green alga (Hao et al., 2019), the different concentration ranges of CMPP-1 and CMPP-2 were used in the following study.

3.8. Immune-enhancing activity

Macrophage activation was an important step in immune defense, enhancing the secretion of cytokines (NO, IL-6 and TNF-α) (Liao et al., 2015). It was commonly used in evaluating the immunomodulatory

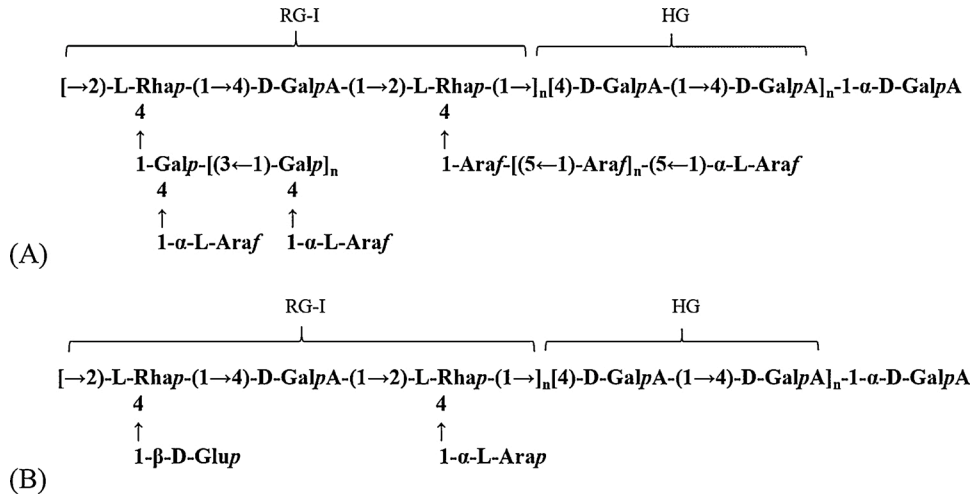

Fig. 5. Predicted structure of CMPP-1 (A) and CMPP-2 (B).

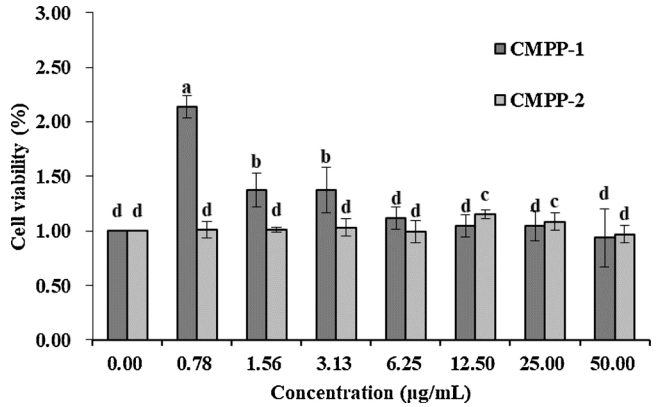

Fig. 6. Effects of CMPP-1 and CMPP-2 on the proliferation. Data were presented as mean ± SD. Different lowercase alphabet letters (a–d) were significantly different if $p < 0.05$.

activity (Lin, Liao, & Ren, 2016).For the release of NO (Fig. 7A–B), it can be seen that NO production was significant increased ($p < 0.05$) in a dose-dependent manner by the treatment of different concentrations of CMPP-1 (3.13–50 μg/mL) and CMPP-2 (6.25−50 μg/mL). Compared with the minimum effective concentration (3.13 μg/mL) of CMPP-1, CMPP-2 showed weaker ability to increase NO production at 6.25 μg/mL. Under the maximum treated concentration (50 μg/mL) of CMPP-1 and CMPP-2, the NO productions were 22.51 μmol/L and 21.58 μmol/L, respectively, which were inferior to the LPS group (33.47μg/mL).Since the over production of NO could cause apoptosis in macrophages (Song et al., 2020), the above results indicated that the two fractions were more moderate than LPS.

As for the secretion of TNF-α and IL-6, ELISA results suggested that the cellular release was also increased with the concentration-dependent manner at the treated concentrations of CMPP-1 and CMPP-2. The production of TNF-α in CMPP-1 (0.78, 3.13, 12,5 and 50 μg/mL) was measured to be 2.6-fold, 4.1-fold, 7.3-fold and 10.2-fold of control group (Fig. 7C). While that of CMPP-2 (6.26, 12.5. 25, 50 μg/mL) was measured to be 2.0-fold, 2.6-fold, 4.4-fold and 7.0-fold of control group (Fig. 7D). Additionally, the lower dosage (6.26 and 12.5 μg/mL) of CMPP-2 treatment showed no significant effect on RAW264.7 cells compared with control group, whereas the higher dosages (25 and 50 μg/mL) exhibited favorable effect on IL-6 (Fig. 7F). Hence, CMPP-1 had wider concentration range (0.78–50 μg/mL) of significant enhancing IL-6 secretion (Fig. 7E) than CMPP-2 (25–50 μg/mL).These results confirmed that CMPP-1 and CMPP-2 could play an immunomodulatory role in secreting NO, TNF-α and IL-6, and CMPP-1 had better immune-enhancing activity than CMPP-2 at the same concentration. The difference in immune activity of the fractions was related to structure, which were in agreement with the previous studies on pectin polysaccharide obtained from citrus (Park et al., 2019), mulberry (Lee et al., 2013) and sweet cherry (Cao et al., 2018).

Immune-enhancing activity is one of the most important activities of pectin polysaccharides, and it is related to the structural characteristics, such as monosaccharide composition, branch degrees and glycosidic linkages, etc. (Borazjani, Tabarsa, You, & Rezaei, 2017) In this study, CMPP-1 and CMPP-2 can be considered as immunostimulatory pectin with the less contain of galacturonic acid (45.93 % and 51.75 %, respectively) and a large branched region with Rha, Gal and Ara, which consistent with these results of pectin from *bergenan*, *silenan*, *butomusan*, and *lemnan* (Popov and Ovodov, 2013). Especially, the immunomodulatory activity of CMPP-1 was higher than that of CMPP-2, and it might be due to the branch region consisting of different ratio of monosaccharide and glycoside bonds. This phenomenon was in accordance with the study on mulberry polysaccharides, which reported that PFA-1 had higher Gal and Ara content than PFA-2 exhibited higher immune activity (Wang, Li et al., 2018). Thus, although the total cellular stimulating activity of pectin was not only controlled by a single structural characteristic (Bahramzadeh et al., 2019), the different of structural features like CMPP-1 and CMPP-2 might be the reasons for their immunomodulatory effect. The structure-activity relationship of pectin polysaccharide needs further study.

4. Conclusions

Taken together, combining hot-water extraction, ethanol precipitation and column chromatography, the present study provided information about two pectin polysaccharides that were isolated from the kiwano peels. According to the results of structural characterization, CMPP-1 and CMPP-2 were acidic heteropolysaccharide fraction and rich in galacturonic acid. The structure of the two fractions were deduced to be RH-I domain with glycan side chains composed of arabinose and galactose, and CMPP-1 possessed higher degree of branching than CMPP-2. Moreover, the two fractions showed immune-enhancing activity and could enhance the secretion of NO and cytokines (TNF-α, IL-6)

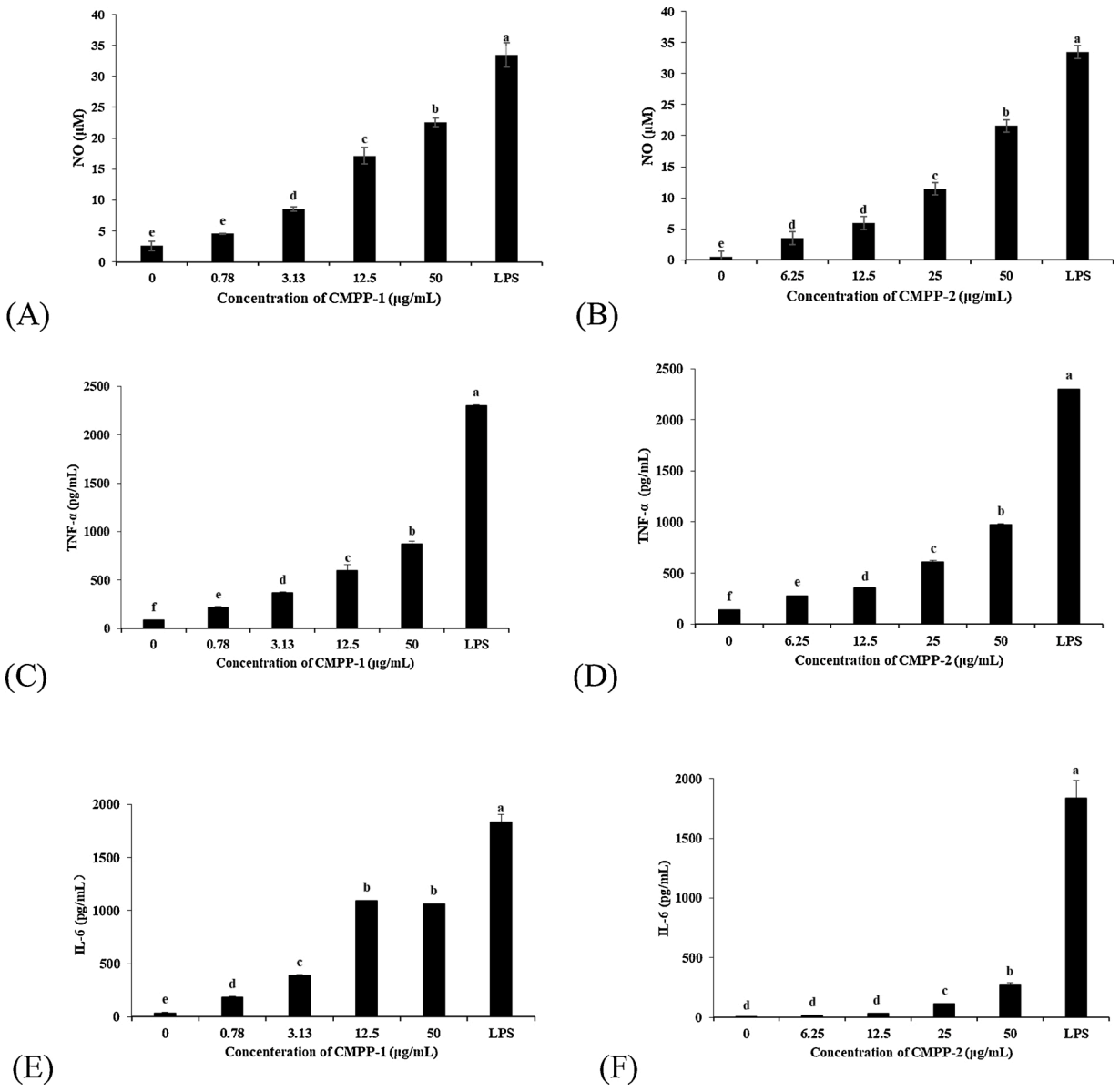

Fig. 7. NO release detection of RAW264.7 cell activation in CMPP-1 and CMPP-2 (A-B). Elisa detection of TNF-α (C-D) and IL-6 (E-F). Data were presented as mean ± SD. Different lowercase alphabet letters (a–e) were significantly different if $p < 0.05$.

in a dose-dependent manner, of which, CMPP-1 had highly immune activity than CMPP-2. From the above results, the polysaccharides from kiwano (*Cucumis metuliferus*) peels could be further developed for utilization.

Declaration of Competing Interest

The authors report no declarations of interest.

Acknowledgements

This work was financially supported by, Key Area R&D Program of Guangdong Province (NO. 2019B020211002), National Natural Science Foundation of China (NO. 32001631), Guangdong Province Universities and Colleges Pearl River Scholar Funded Scheme (2017), International Cooperation Program of SCAU (NO. 2019SCAUGH03).

Appendix A. Supplementary data

Supplementary material related to this article can be found, in the online version, at doi:https://doi.org/10.1016/j.carbpol.2020.117371.

References

Anyanwu, A., & Wannang, N. (2014). Alkaloids of the fruit pulp of *cucumis metuliferus e. Meye* (cuecubitaceae) have antiviral activity against ibdv and ndv. *Basic & Clinical Pharmacology & Toxicology, 115*(1), 1–347.

Bahramzadeh, S., Tabarsa, M., You, S., Yelithao, K., Klochkov, V., & Ilfat, R. (2019). An arabinogalactan isolated from *boswellia carterii*: Purification, structural elucidation and macrophage stimulation via nf-κb and mapk pathways. *Journal of Functional Foods, 52*, 450–458.

Bi, S., Jing, Y., Zhou, Q., Hu, X., Zhu, J., Guo, Z., et al. (2018). Structural elucidation and immunostimulatory activity of a new polysaccharide from *cordyceps militaris*. *Food & Function, 9*, 279–293.

Borazjani, N. J., Tabarsa, M., You, S., & Rezaei, M. (2017). Effects of extraction methods on molecular characteristics, antioxidant properties and immunomodulation of alginates from *sargassum angustifolium*. *International Journal of Biological Macromolecules, 101*, 703–711.

Cao, J. P., Tang, D. D., Wang, Y., Li, X., Hong, L., & Sun, C. D. (2018). Characteristics and immune-enhancing activity of pectic polysaccharides from sweet cherry (*prunus avium*). *Food Chemistry, 254*, 47–54.
Chen, S., Huang, H., & Huang, G. (2019). Extraction, derivatization and antioxidant activity of cucumber polysaccharide. *International Journal of Biological Macromolecules, 140*, 1047–1053.
Dammak, M. I., Ben Salem, Y., Belaid, A., Ben Mansour, H., Hammami, S., Le Cerf, D., et al. (2019). Partial characterization and antitumor activity of a polysaccharide isolated from watermelon rinds. *International Journal of Biological Macromolecules, 136*, 632–641.
Denman, L. J., & Morris, G. A. (2015). An experimental design approach to the chemical characterisation of pectin polysaccharides extracted from *cucumis melo inodorus*. *Carbohydrate Polymers, 117*, 364–369.
Du, J., Li, J. J., Zhu, J. H., Huang, C. H., Bi, S. X., Song, L. Y., et al. (2018). Structural characterization and immunomodulatory activity of a novel polysaccharide from *ficus carica*. *Food & Function, 9*(7), 3930–3943.
Dubois, M., Gilles, K. A., Hamilton, J. K., Rebers, P. A., & Smith, F. (1956). Colorimetric method for determination of sugars and related substances. *Analytical Chemistry, 28*, 350–356.
Feng, J., YuRong, G., Xi, Y., Dong, L., & Jie, L. (2017). Isolation and purification of polysaccharide from fermented apple pomace and its relationship with processing characteristics. *Scientia Agricultura Sinica, 50*(10), 1873–1884.
Freysdottir, J., Logadottir, O. T., Omarsdottir, S. S., Vikingsson, A., & Hardardottir, I. (2016). A polysaccharide fraction from *achillea millefolium* increases cytokine secretion and reduces activation of akt, erk and nf-κb in thp-1 monocytes. *Carbohydrate Polymers*, Article S014486171630073X.
Gavlighi, H. A., Tabarsa, M., You, S., Surayot, U., & Ghaderi-Ghahfarokhi, M. (2018). Extraction, characterization and immunomodulatory property of pectic polysaccharide from pomegranate peels: Enzymatic vs conventional approach. *International Journal of Biological Macromolecules, 116*, 698–706.
Gotep, J. (2011). Glycosides fraction extracted from fruit pulp of *cucumis metuliferus e. Meyer* has antihyperglycemic effect in rats with alloxan-induced diabetes. *Journal of Natural Pharmaceuticals, 2*(2), 48–51.
Hao, H., Han, Y., Yang, L., Hu, L., Duan, X., Yang, X., et al. (2019). Structural characterization and immunostimulatory activity of a novel polysaccharide from green alga *caulerpa racemosa var peltata*. *International Journal of Biological Macromolecules, 134*, 891–900.
Hazime, S., Yoshioka, Y., Uehara, N., Aketagawa, J., Tanaka, S., & Shibata, Y. (1991). Relationship between conformation and biological response for (1→3)-β-d-glucans in the activation of coagulation factor g from limulus amebocyte lysate and host-mediated antitumor activity. Demonstration of single-helix conformation as a stimulant. *Carbohydrate Research, 217*, 181–190.
Jiao, Y., Hua, D., Dong, H., Qian, Z., & Yan, C. (2018). Characterization of a new heteropolysaccharide from green guava and its application as an α-glucosidase inhibitor for the treatment of type ii diabetes. *Food & Function, 9*(7), 3997–4007.
Jiao, Y. C., Kuang, H., Hu, J. J., & Chen, Q. H. (2018). Structural characterization and anti-hypoxia activities of polysaccharides from the sporocarp, fermentation broth and cultured mycelium of *agaricus bitorquis (quel.) sacc*. Chaidam in mice. *Journal of Functional Foods, 51*, 75–85.
Kazemi, M., Khodaiyan, F., Labbafi, M., Hosseini, S. S., & Hojjati, M. (2019). Pistachio green hull pectin: Optimization of microwave-assisted extraction and evaluation of its physicochemical, structural and functional properties. *Food Chemistry, 271*, 663–672.
Lee, J. S., Synytsya, A., Kim, H. B., Choi, D. J., Lee, S., Lee, J., et al. (2013). Purification, characterization and immunomodulating activity of a pectic polysaccharide isolated from korean mulberry fruit *oddi (morus alba l.)*. *International Immunopharmacology, 17*(3), 858–866.
Lei, W., Chen, C., Zhang, B., Qiang, H., Xiong, F., & Chao, L. (2018). Structural characterization of a novel acidic polysaccharide from *rosa roxburghii* tratt fruit and its α-glucosidase inhibitory activity. *Food & Function, 9*, 3974–3985.
Li, J., Zhong, Y., & Liu, C. (2010). Purification and electronmicroscope analysisof *lentinan*. *Journal of Shanxi Agricultural Sciences, 38*(3), 6–9.
Liao, W. Z., Luo, Z., Liu, D., Ning, Z. X., Yang, J. G., & Ren, J. Y. (2015). Structure characterization of a novel polysaccharide from *dictyophora indusiata* and its macrophage immunomodulatory activities. *Journal of Agricultural and Food Chemistry, 63*(2), 535–544.
Lin, Z. H., Liao, W. Z., & Ren, J. Y. (2016). Physicochemical characterization of a polysaccharide fraction from *platycladus orientalis (l.) franco* and its macrophage immunomodulatory and anti-hepatitis b virus activities. *Journal of Agricultural and Food Chemistry, 64*(29), 5813–5823.
Liu, Q., & Xu, X. (2016). Recent progress in chain conformation and function of triple helical polysaccharides. *Journal of Functional Polymer, 29*(2), 134–152.
Liu, J., Zhao, Y., Wu, Q., John, A., & Yang, B. (2017). Structure characterisation of polysaccharides in vegetable' okra' and evaluation of hypoglycemic activity. *Food Chemistry, 242*, 211–216.
Liu, W., Liu, Y., Zhu, R., Yu, J., & Gaoa, X. (2016). Structure characterization, chemical and enzymatic degradation, and chain conformation of an acidic polysaccharide from *lycium barbarum l. Carbohydrate Polymers, 147*, 114–124.
Matsusaka, Y., & Kawabata, J. (2010). Evaluation of antioxidant capacity of non-edible parts of some selected tropical fruits. *Food Science and Technology Research, 16*(5), 467–472.
Mei, Y. X., Yang, W., Zhu, P. X., Peng, N., & Liang, Y. X. (2014). Isolation, characterization, and antitumor activity of a novel heteroglycan from cultured mycelia of *cordyceps sinensis*. *Planta Medica, 80*(13), 1107–1112.
Mohnen, D. (2008). Pectin structure and biosynthesis. *Current Opinion in Plant Biology, 11*(3), 266–277.
Molaei, H., & Jahanbin, K. (2018). Structural features of a new water-soluble polysaccharide from the gum exudates of *amygdalus scoparia spach (zedo gum)*. *Carbohydrate Polymers, 182*, 98–105.
Morrison, D. C., & Jacobs, D. M. (1976). Binding of polymyxin b to the lipid a portion of bacterial lipopolysaccharides. *Immunochemistry, 13*(10), 813–818.
Nwadiaro, P. O., Ogbonna, A. I., Wuyep, P. A., & Sila-Gyang, M. D. (2015). Antifungal activity of *cucumis metuliferus e.Mey. Ex naudin* on some post-harvest decay fungi of string beans. *Journal of Academia and Industrial Research, 3*(10), 490–496.
Omale, S., Wuyep, N. N., Auta, A., & Wannang, N. N. (2011). Anti-ulcer properties of alkalodis isoated from the fruit pulp of *cucumis metuliferous (curcurbitaceae)*. *International Journal of Pharmaceutical Sciences and Research, 2*(10), 2586–2588.
Park, H. R., Lee, S. J., Im, S. B., Shin, M. S., Choi, H. J., Park, H. Y., et al. (2019). Signaling pathway and structural features of macrophage-activating pectic polysaccharide from Korean citrus, *cheongkyool* peels. *International Journal of Biological Macromolecules, 137*, 657–665.
Popov, S. V., & Ovodov, Y. S. (2013). Polypotency of the immunomodulatory effect of pectins. *Biochemistry-Moscow, 78*(7), 823–835.
Rahmani, Z., Khodaiyan, F., Kazemi, M., & Sharifan, A. (2019). Optimization of microwave-assisted extraction and structural characterization of pectin from sweet lemon peel. *International Journal of Biological Macromolecules, 147*, 1107–1175.
Ren, D. Y., Zhao, Y., Zheng, Q., Alim, A., & Yang, X. B. (2019). Immunomodulatory effects of an acidic polysaccharide fraction from herbal *gynostemma pentaphyllum* tea in raw264.7 cells. *Food and Function, 10*(4), 2186–2197.
Shu, Z. P., Yang, Y. N., Xing, N., Wang, Y., Wang, Q. H., & Kuang, H. X. (2018). Structural characterization and immunomodulatory activity of a pectic polysaccharide (calb-4) from *fructus aurantii*. *International Journal of Biological Macromolecules, 116*, 831–839.
Song, Y., Wen, P., Hao, H., Zhu, M., Sun, Y., Zou, Y., et al. (2020). Structural features of three hetero-galacturonans from *passiflora foetida* fruits and their in vitro immunomodulatory effects. *Polymers, 12*, 1–21.
Song, Y., Zhu, M., Hao, H., Deng, J., Li, M., Sun, Y., et al. (2019). Structure characterization of a novel polysaccharide from chinese wild fruits (*passiflora foetida*) and its immune-enhancing activity. *International Journal of Biological Macromolecules, 136*, 324–331.
Ullah, S., Khalil, A. A., Shaukat, F., & Song, Y. D. (2019). Sources, extraction and biomedical properties of polysaccharides. *Foods, 8*(8), 23.
Wang, W. J., Ma, X. B., Jiang, P., Hu, L. L., Zhi, Z. J., Chen, J. L., et al. (2016). Characterization of pectin from grapefruit peel: A comparison of ultrasound-assisted and conventional heating extractions. *Food Hydrocolloids, 61*, 730–739.
Wang, D. X., Li, H., Li, B., Ma, R., Zhang, N., Zhang, X. Y., et al. (2018). Systematic fractionation and immunoenhancement of water-soluble polysaccharides isolated from fruit of *morus alba l. International Journal of Biological Macromolecules, 116*, 1056–1063.
Wang, Y., Zheng, W., Cai, J., Yuan, T., & Gong, X. (2018). Structural analysis and anti-pancreatic lipase activity of flavonoids from *moringa oleifera lam.* leaves. *Food Science, 39*, 31–37.
Wei, C., Zhang, Y., He, L., Cheng, J., Li, J., Tao, W., et al. (2019). Structural characterization and anti-proliferative activities of partially degraded polysaccharides from peach gum. *Carbohydrate Polymers, 203*, 193–202.
Yang, J., Wen, L., Zhao, Y., Jiang, Y., Tian, M., Liu, H., et al. (2018). Structure identification of an arabinogalacturonan in citrus reticulata blanco "chachiensis" peel. *Food Hydrocolloids, 84*(NOV), 481–488.
Yi, W., Li, Y., Liu, C., Li, E., Gao, Z., Liu, C., et al. (2016). Structural characterization of an acidic epimedium polysaccharide and its immune-enhancement activity. *Carbohydrate Polymers, 138*, 134–142.
Zeng, Y. J., Yang, H. R., Wang, H. F., Zong, M. H., & Lou, W. Y. (2019). Immune enhancement activity of a novel polysaccharide produced by *dendrobium* officinale endophytic fungus *fusarium solani do7*. *Journal of Functional Foods, 53*, 266–275.
Zhang, J. X., Chen, M., Wen, C. T., Zhou, J., Gu, J. Y., Duan, Y. Q., et al. (2019). Structural characterization and immunostimulatory activity of a novel polysaccharide isolated with subcritical water from *sagittaria sagittifolia l. International Journal of Biological Macromolecules, 133*, 11–20.
Zhang, W. S., Li, X., Zheng, J. T., Wang, G. Y., Sun, C. D., Ferguson, I. B., et al. (2008). Bioactive components and antioxidant capacity of chinese bayberry (*myrica rubra sieb. And zucc.*) fruit in relation to fruit maturity and postharvest storage. *European Food Research and Technology, 227*(4), 1091–1097.
Zhao, T., Mao, G., Feng, W., Mao, R., Xiaoyun, G., Li, T., et al. (2014). Isolation, characterization and antioxidant activity of polysaccharide from *schisandra sphenanthera*. *Carbohydrate Polymers, 105*, 26–33.